

Supplemental information titles and legends:

Endometrial cells with high ALDH activity contribute to uterine development and regeneration

Suni Tang^{1,2}; Anna Catherine Unser^{1,2}; Peixin Jiang¹; Sydney E. Parks^{1,2}; Genesis J. Herrera^{1,2}; Ting Geng^{1,2}; Linda Alpuing Radilla³; Brooke A. Thigpen³; Xiaoming Guan³; Diana Monsivais^{1,2}

1. Department of Pathology & Immunology, Baylor College of Medicine, Houston, Texas, USA
2. Center for Drug Discovery, Baylor College of Medicine, Houston, Texas, USA
3. Department of Obstetrics and Gynecology, Baylor College of Medicine, Houston, Texas, USA

SUPPLEMENTARY TABLES

Table S1. Differentially expressed genes and gene enrichment analysis of ALDH^{HI} vs. ALDH^{LO} mouse endometrial epithelial organoids.

Table S2. Differentially expressed genes between clusters 4 and 25 versus other epithelial cell clusters in the scRNAseq dataset.

Table S3. Differentially expressed genes and gene enrichment analysis of ALDH^{HI} vs. ALDH^{LO} human endometrial epithelial organoids.

Table S4. Primer sequences and antibody information.

Table S5. Patient sample information.

FIGURE LEGENDS

Figure S1. Analysis of DEG in ALDH^{HI} vs. ALDH^{LO} mouse organoids. Clustering analysis of stemness-related (A) and keratin genes (C) in the mouse epithelial cells established from ALDH^{HI} or ALDH^{LO} organoids. B) Overlap of ALDH^{HI} genes that are increased and decreased with AXIN2^{HI} endometrial epithelial stem cells in mouse.

Figure S2. Identification and characterization of epithelial stem cells in the adult WT mouse uterus at estrus and diestrus. A) Dot plots showing the expression of *Aldh1a1*, *Lgr5*, and *Axin2* across the epithelial cell subclusters from the estrus and diestrus phases. B) Estrus and diestrus phase expression of genes identifying epithelial, luminal, and epithelial stem cell clusters across each cluster of epithelial cells. C) Heatmap (row for gene, column for individual cell) comparing epithelial cell subclusters from our dataset to DEGs identified from EpSC DEGs of cluster 12 (Padilla-Banks et al., 2023). D) UMAP of epithelial cell subclusters from mouse samples obtained during the estrus (E) or diestrus phases (F). F-L) Lineage trajectories using pseudotime analysis of the epithelial cell types in estrus (F,G) and diestrus (H-L).

Figure S3. Estrogen and progesterone impact the expression and localization of ALDH1A1 in the WT mouse uterus. A) Description of the experimental scheme used to ovariectomize and administer hormonal treatments to 6-8-week-old WT mice. B-E') ALDH1A1 immunohistochemistry in the uterine cross-sections of ovariectomized mice treated with vehicle (B-B'), 1mg P4 (C-C'), 50ng E2 (D-D'), or 1mg P4 + 50ng E2 (E-E'). F) *Aldh1a1* gene expression was quantified in the uterine tissues of the ovariectomized mice treated with Vehicle, P4, E2 or E2 + P4. Experiments were repeated in more than three mice per group. Data in F displayed as mean \pm SEM analyzed by a One-Way ANOVA test with a Tukey's post-hoc test. *, $p < 0.05$; **, $P < 0.01$; ***, $p < 0.001$. G-H') Immunohistochemistry of the uterus of mice collected 4 days after DT administration in control, DTR^{flox/flox} (G-G') and DTR^{flox/flox}; *Aldh1a1*^{cre/ERT2} (H-H') mice.

Figure S4. ALDH1A1+ cells in the regenerating endometrium during the postpartum phase. A-F) RFP immunohistochemistry in the placental detachment sites of mice collected at postpartum day 1 (PPD1) (A-B'), PPD3 (C-D'), and PPD5 (E-F'). G) Quantification of the RFP⁺ epithelial and stromal cells at PPD1, PPD3, and PPD5. Graph shows mean \pm SEM.

Figure S5. Comparison of ALDH^{HI} and ALDH^{LO} formation in the organoids from human eutopic endometrial epithelium. A-B) Phase contrast images and quantification of an organoid formation assay comparing ALDH^{HI} and ALDH^{LO} cells. Data in C are displayed as mean \pm SD analyzed by a two-tailed t-test. *, $p < 0.05$; **, $P < 0.01$; ***, $p < 0.001$. Data are from one patient performed in technical replicates.

Figure S6. Gene expression pathways are differentially regulated between ALDH^{HI} and ALDH^{LO} cells in the eutopic endometrial organoids. Clustering of the top 100 differentially expressed genes in ALDH^{HI} vs ALDH^{LO} human eutopic endometrial epithelial organoids.

Figure S7. Genotyping strategy for the various mouse lines used in the study. A-E) Gel electrophoresis results showing the PCR results for the *Aldh1a1*^{cre/ERT2} allele (A), for the Ai9/Ai9^{tdTomato} reporter (B) and for the DTR knock-in and WT alleles (E).

Figure S1

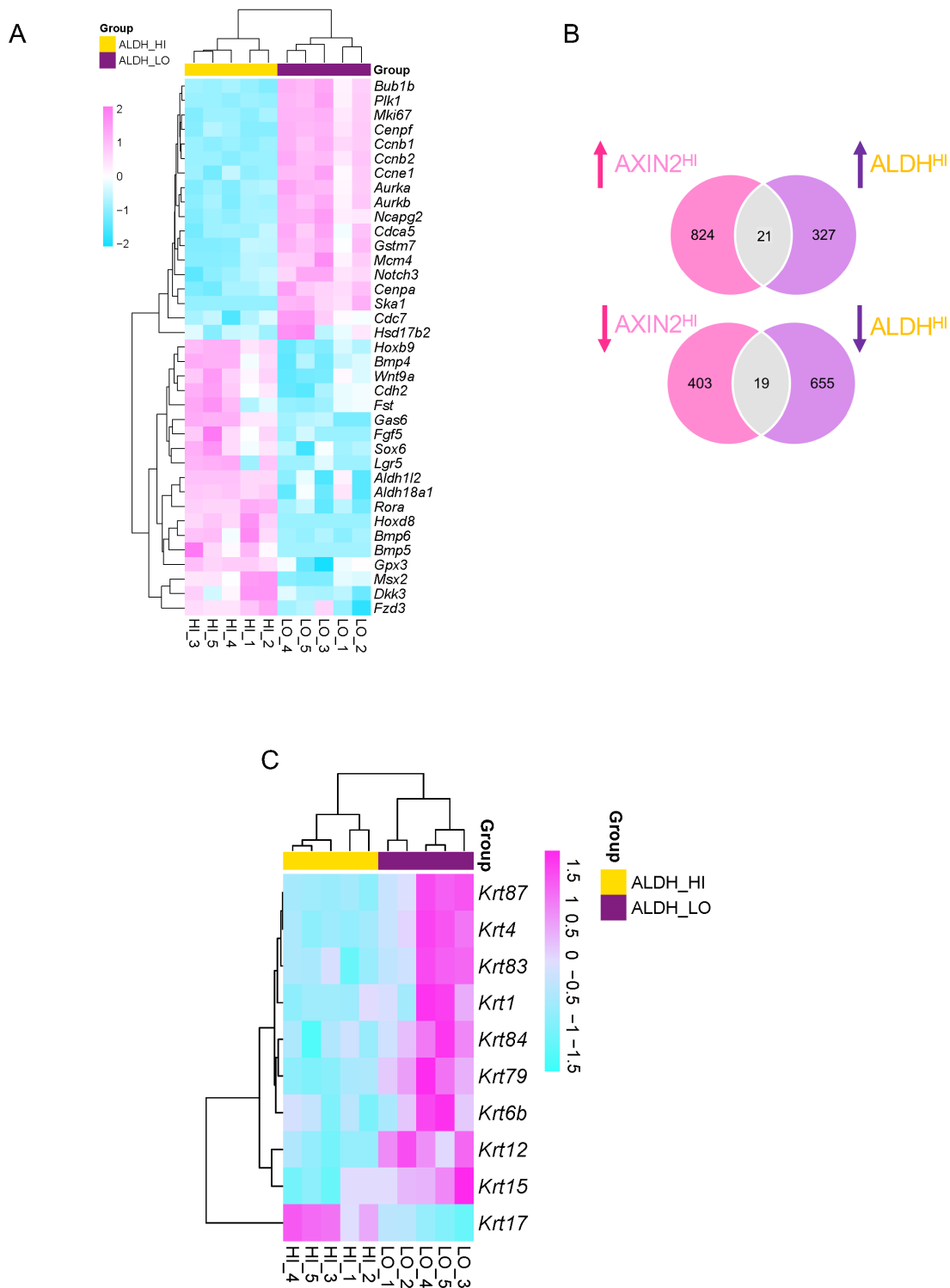


Figure S2

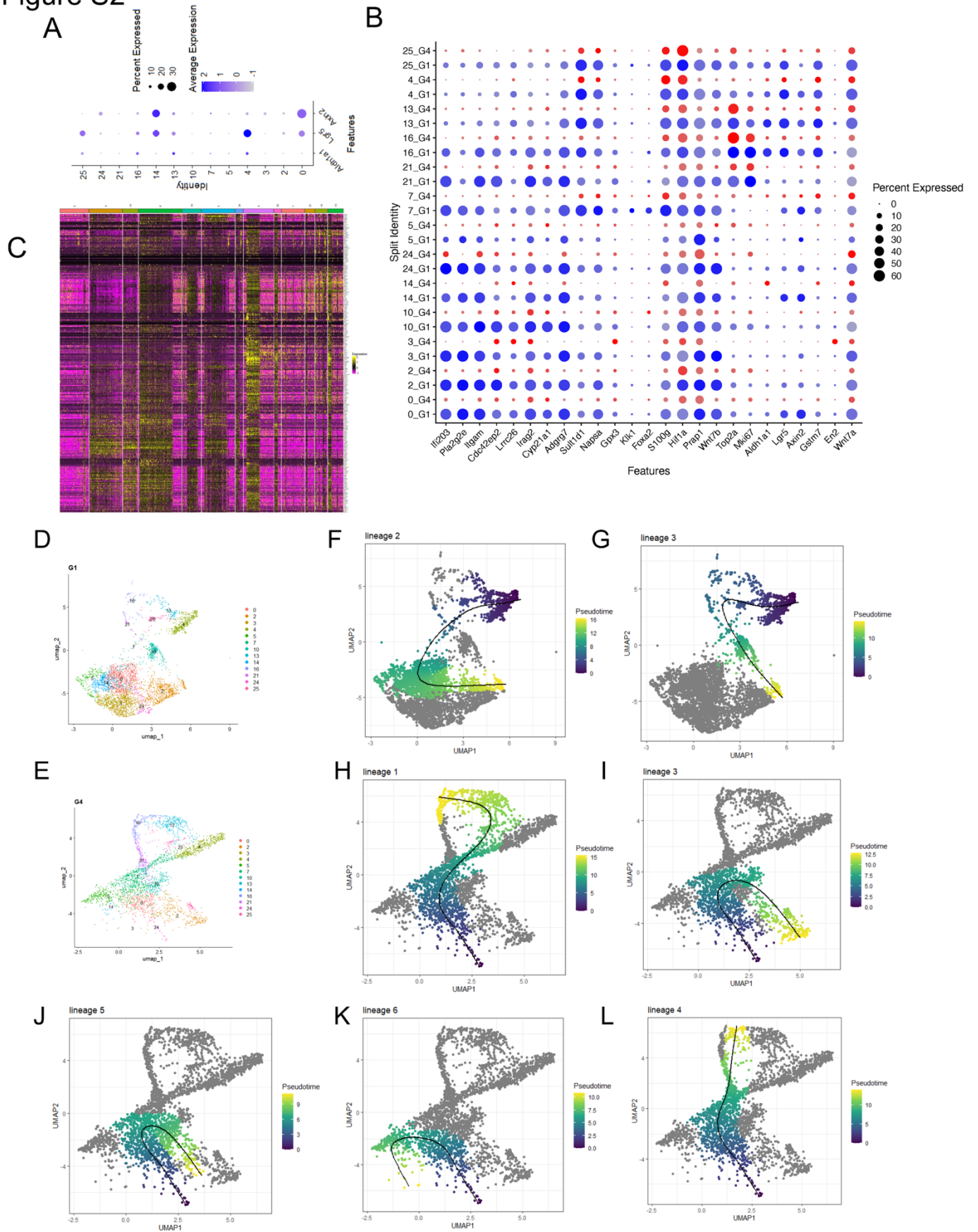


Figure S3

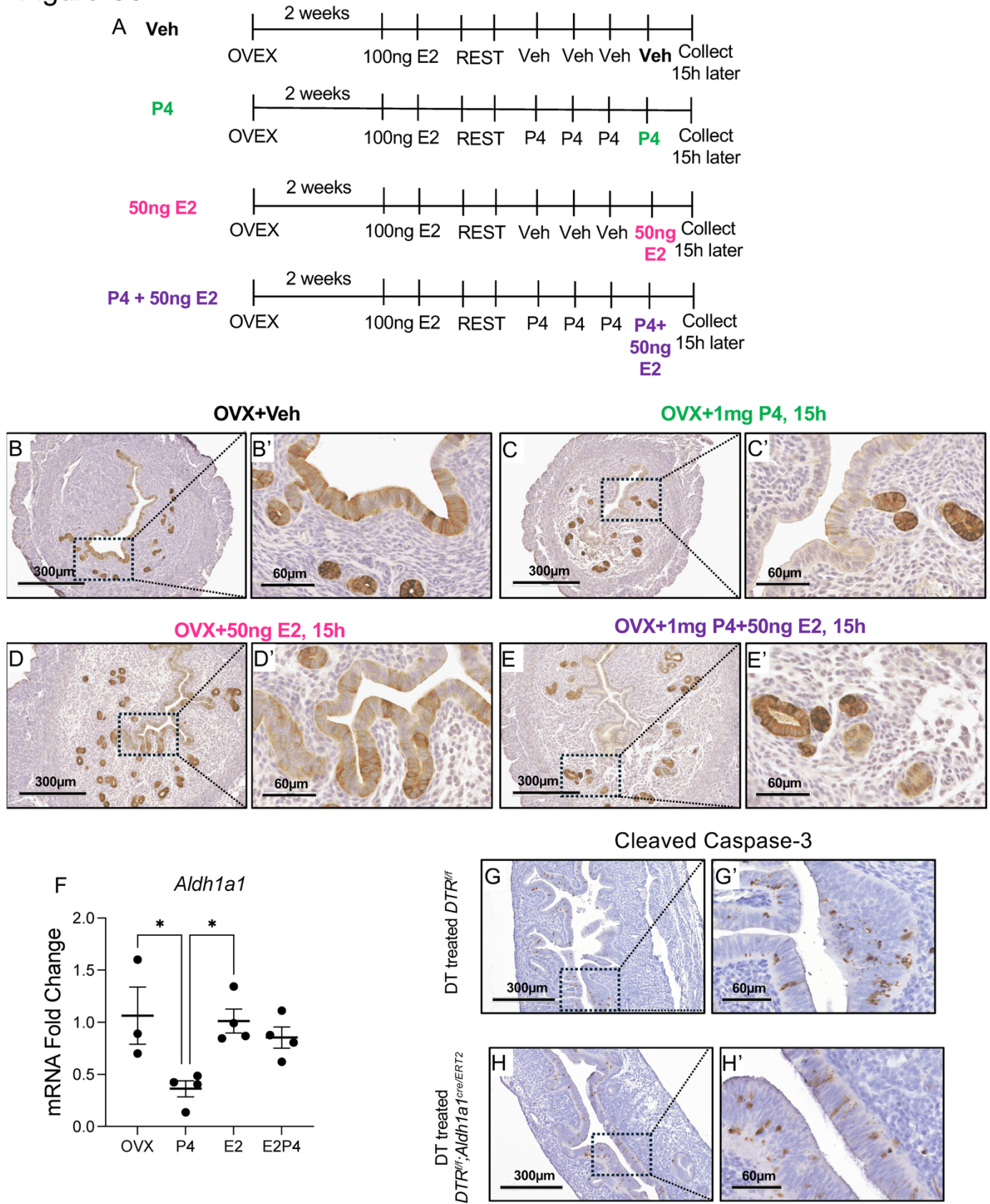


Figure S4

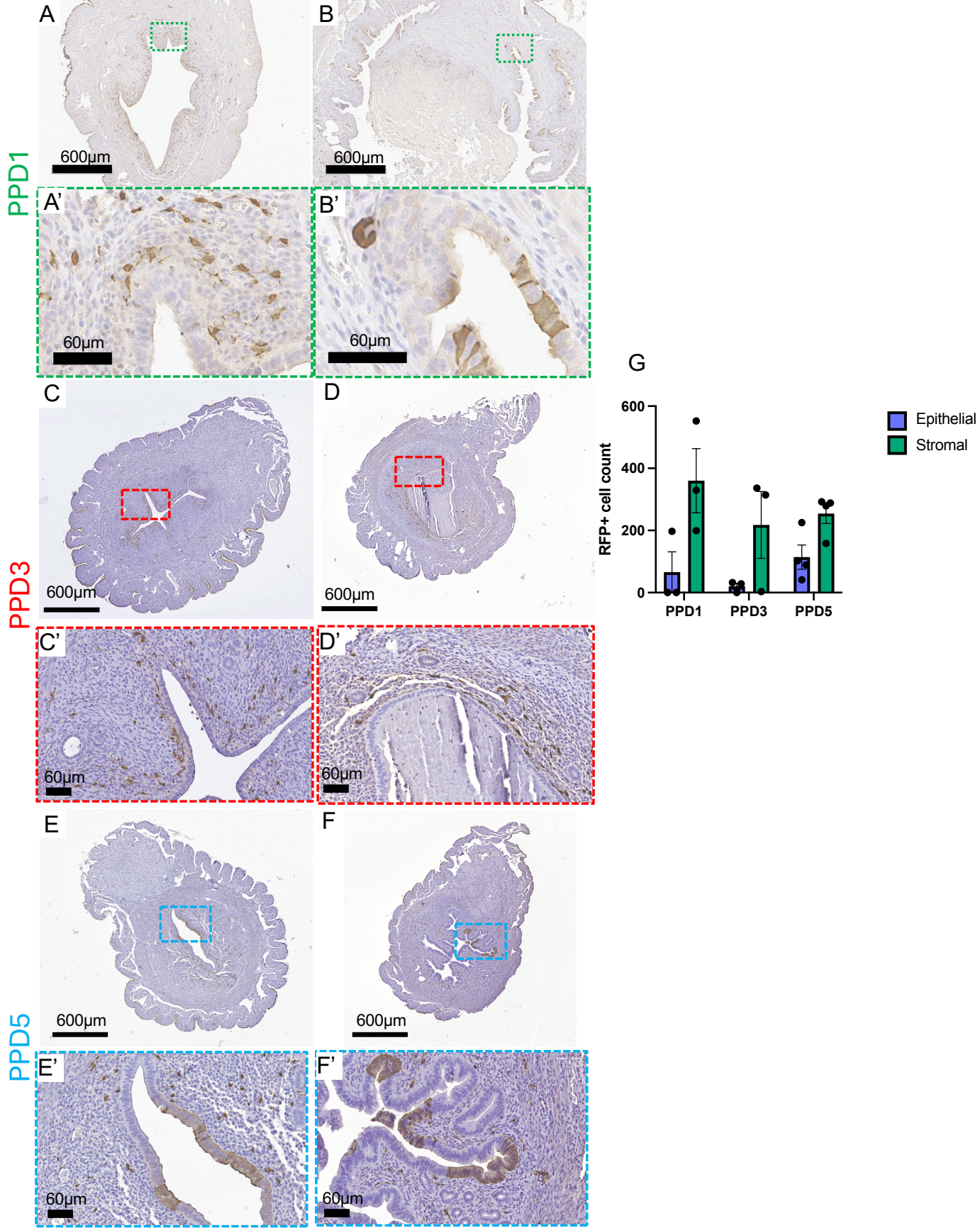
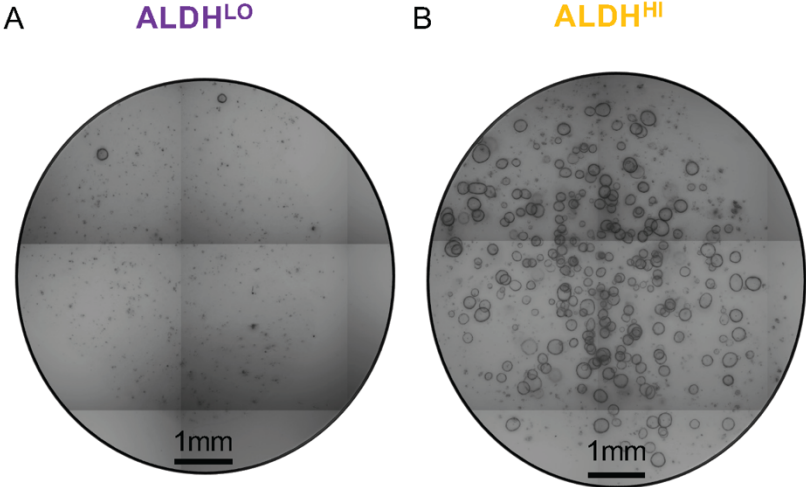


Figure S5



C

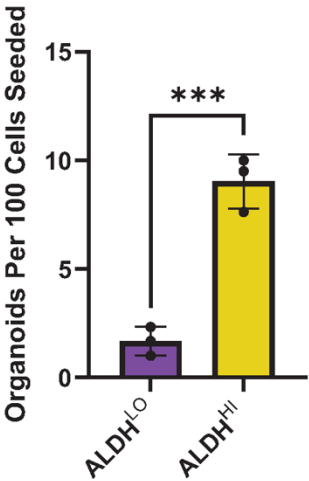
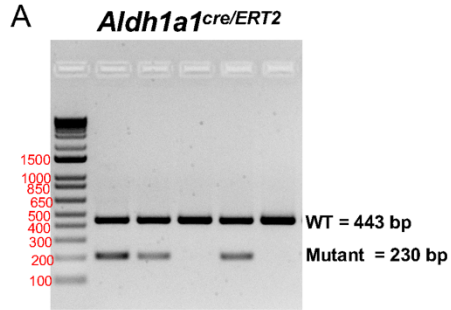


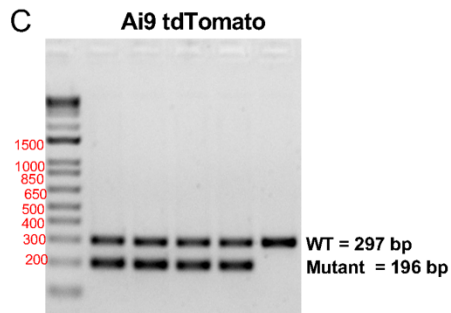
Figure S7

Genotyping information for *Aldh1a1*^{cre/ERT2}, Ai9 tdTomato, and DTR alleles



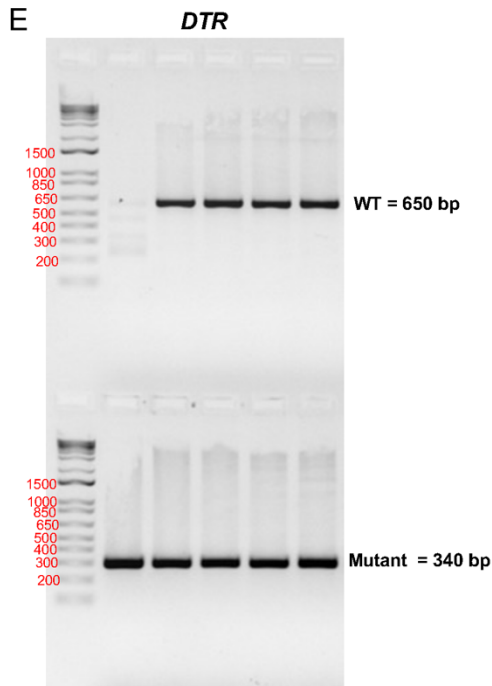
B *Aldh1a1*^{cre/ERT2}

Step	Temp °C	Time
1	94	4 min
2	94	30 sec
3	60	30 sec
4	72	35 sec
5	Repeat steps 2-4 for 34 cycles	
6	72	5 min
7	16	hold



D Ai9 tdTomato / DTR

Step	Temp °C	Time	Note
1	94	2 min	
2	94	20sec	
3	65	15sec	-0.5 C per cycle decrease
4	68	10sec	
5	Repeat steps 2-4 for 10 cycles (Touchdown)		
6	94	15sec	
7	60	15sec	
8	72	10sec	
9	Repeat steps 6-8 for 28 cycles		
10	72	2 min	
11	10	hold	



Supplementary Table S4. List of primers and antibodies

Genotyping Primers	Forward Primer (5'-3')	Reverse Primer (5'-3')
<i>Aldh1a1</i> ^{cre/ERT2} (promoter)	AGTCTGCCCATCCAATCATATC	
<i>Aldh1a1</i> ^{cre/ERT2} (<i>Aldh1a1</i>)	TCTATGGTTCACCTGCACTCTGG	
<i>Aldh1a1</i> ^{cre/ERT2} (Cre)	GTTCTTGCGAACCTCATCACTC	
Ai9 tdTomato (oIMR9020)	AAGGGAGCTGCAGTGGAGTA	
Ai9 tdTomato (oIMR9021)	CCGAAAATCTGTGGGAAGTC	
Ai9 tdTomato (oIMR9103)	GGCATTAAAGCAGCGTATCC	
Ai9 tdTomato (oIMR9105)	CTGTTCTGTACGGCATG G	
DTR (mutant)		GCGAAGAGTTTGTCTCAACC
DTR (common)	AAAGTCGCTCTGAGTTGTTAT	
DTR (WT)		GGAGCGGGAGAAATGGATATG
PCR Primers	Forward Primer (5'-3')	Reverse Primer (5'-3')
<i>Aldh1a1</i>	ATACTTGTCCGATTTAGGAGGCT	GGGCCTATCTTCCAATGAACA
<i>Gapdh</i>	CAATGTGTCCGTCGTGGATCT	GCCTGCTTCACCACCTTCTT
<i>Rpl17</i>	ACCGCACTGAGATTCGGATG	GAACCTTACGAACCATTTGGGC
<i>Hprt</i>	GTGATTAGCGATGATGAACCA	GCAAGTCTTTTCAGTCCTGTC
Antibody Name	Vendor and Catalog#	Dilution used
ALDH1A1	Abcam, ab52492	1:50 (IHC)
Ki-67	BD Pharmingen, 550609	1:500 (IHC)
cleaved caspase-3	Cell Signaling, 9661	1:400 (IHC)
RFP	Rockland, 600-401-379	1:500 (IHC)
RFP	Abcam, ab125244	1:200 (IF)
FOXA2	Abcam, ab108422	1:200 (IHC), 1:50 (IF)
Cytokeratin 8	DSHB, TROMA-1	1:50 (IF)
Vimentin	Cell Signaling, 5741	1:200 (IF)
Phospho Histone H3	Abcam, ab5176	1:200 (IF)
Acetyl- α -Tubulin	Cell Signaling, 5335	1:200 (IF)
Anti-Rabbit IgG Antibody	Vector Laboratories, BA-1000	1:200 (IHC)
Anti-Mouse IgG Antibody	Vector Laboratories, BA-9200	1:200 (IHC)
Anti-Rat IgG (H+L), AF488	Invitrogen, A-21208	1:250 (IF)
Anti-Rabbit IgG (H+L), AF594	Invitrogen, A-21207	1:250 (IF)
Anti-Mouse IgG (H+L), AF488	Invitrogen, A-21202	1:250 (IF)
Anti-Rabbit IgG (H+L), AF568	Invitrogen, A-10042	1:250 (IF)
Anti-Rat IgG (H+L), AF647	Invitrogen, A78947	1:250 (IF)